

## Stochastic upscaling via linear Bayesian updating

Sadiq M. Sarfaraz<sup>\*1</sup>, Bojana V. Rosić<sup>1a</sup>, Hermann G. Matthies<sup>1b</sup> and  
Adnan Ibrahimbegović<sup>2c</sup>

<sup>1</sup>*Institute of Scientific Computing, Technische Universität Braunschweig  
38106 Braunschweig, Germany*

<sup>2</sup>*Lab. de Mécanique Roberval / Centre de Recherche Royallieu,  
Université de Technologie de Compiègne, 60203 Compiègne, France*

(Received August 23, 2017, Revised September 26, 2017, Accepted September 28, 2017)

**Abstract.** In this work we present an upscaling technique for multi-scale computations based on a stochastic model calibration technique. We consider a coarse-scale continuum material model described in the framework of generalized standard materials. The model parameters are considered uncertain, and are determined in a Bayesian framework for the given fine scale data in a form of stored energy and dissipation potential. The proposed stochastic upscaling approach is independent w.r.t. the choice of models on coarse and fine scales. Simple numerical examples are shown to demonstrate the ability of the proposed approach to calibrate coarse scale elastic and inelastic material parameters.

**Keywords:** Upscaling; Bayesian updating; Gauss-Markov-Kalman filter; coupled plasticity-damage

### 1. Introduction

Many naturally existing or man-made materials such as rock/soils, bones and concrete are known to be heterogeneous on the spatial scales that are orders of magnitudes smaller than the respective scales related to response predictions. Additionally, the micro- and macro-scale models may be of an entirely different mathematical nature as the former ones can be discrete, and the latter ones continuum models. In such a case the classical “homogenization” approaches are known to be insufficient for upscaling purposes as refereed in Ibrahimbegović and Matthies (2012), Matthies and Ibrahimbegović (2014). To bridge the two scales in a more unified manner independent of the class of the mathematical model or the type of heterogeneity, in this paper the stochastic upscaling procedure is considered (Arsigny *et al.* 2006, Clément *et al.* 2013, Ghanem and Das 2011, Demmie and Ostaja-Starzewski 2015, Gorgularslan and Choi 2014, Brady *et al.* 2006, Starzewski 2008, Stefanou *et al.* 2015, Steven *et al.* 2011).

Many researchers have contributed in this field. The common goal is to somehow capture fine

---

\*Corresponding author, E-mail: [m.sarfaraz@tu-bs.de](mailto:m.sarfaraz@tu-bs.de)

<sup>a</sup>Ph.D., E-mail: [bojana.rosic@tu-bs.de](mailto:bojana.rosic@tu-bs.de)

<sup>b</sup>Professor, E-mail: [wire@tu-bs.de](mailto:wire@tu-bs.de)

<sup>c</sup>Professor, E-mail: [adnan.ibrahimbegovic@utc.fr](mailto:adnan.ibrahimbegovic@utc.fr)

scale features in a stochastic setting. Stefanou *et al.* (2015) employed computational homogenization and XFEM to study the effect of uncertainty in material properties and geometrical features on macro-scale. Clément *et al.* (2013) have proposed a strategy to construct stochastic energy functional from realizations of random micro-structure. Brady *et al.* (2006) have utilized a “Moving Window” approach to characterize micro-scale randomness, a similar idea is used to infer meso-scale random fields of material stiffness tensor from bi-phased micro scale by Demmie and Ostaja-Starzewski (2015). Another way to achieve the coupling between scales with possibly completely different descriptions is to use concepts of machine learning as in Koutsourelakis (2007), the theory of which is often, at least conceptually, grounded in Bayesian ideas.

In this paper a Bayesian approach (Kaipio and Somersalo 2004, Kennedy and O’Hagan 2001, Hawkins-Daarud *et al.* 2013) is taken directly in its computationally cheaper Gauss-Markov-Kalman filter form, a generalisation of classical Kalman filtering that allows direct estimation of non-Gaussian distributions without sampling (Pajonk *et al.* 2012, Rosić *et al.* 2012, Rosić *et al.* 2016). The general set-up we propose here is as follows: on the macro scale a continuum material model is derived which not only covers the mean (i.e., homogenised) behavior, but also the possible deviations from it. As the micro-scale mechanical behavior, we have in mind involves both reversible (i.e., elastic) as well as irreversible (i.e., inelastic) behavior, this has to be reflected also in the constitutive models considered on the macro scale. Here the main goal is to show a proof-of-concept, so we will limit ourselves to a simple but sufficiently representative case of inelastic behavior (Liu *et al.* 2013). For the sake of simplicity, we limit ourselves to isothermal conditions and we shall exclude strain-rate dependent behavior. Thus, for the inelastic or irreversible part we only consider ductile non-softening behavior, i.e., strain-rate independent plasticity and damage with hardening. However, one can consider choice of more complex structural/continuum models for upscaling e.g. (Do and Ibrahimbegović 2015, Do *et al.* 2015, Ngo *et al.* 2014, Ngo *et al.* 2014).

As this is to be a model for possibly more complex behavior, we shall assume that the macro-scale continuum model can be described as a generalised standard material model (Halpen and Nguyen 1974, Halpen and Nguyen 1975, Nguyen, 1977). This has the advantage that these materials are completely characterized by the specification of two scalar functions, the stored energy resp. Helmholtz free energy, and the dissipation pseudo-potential. In this way the simple case chosen here can be generalized to very complex material behavior. In our view this description is also a nice and simple illustration for the connection with the micro-scale behavior. No matter how the physical and mathematical/computational description on the micro scale has been chosen, in all cases where the description is based on physical principles it will be possible to define the stored (Helmholtz free) energy and the dissipation (entropy production). These two thermodynamic functions will thus be used as measurements in Bayesian inference to identify the macro-scale model parameters given micro-scale response energy.

In some more detail, the identification of the macro-structure generalized standard material constitutive model proceeds as follows: the micro-structure is exposed to some external action resp. stimulus, here purely mechanical case this is chosen as large scale homogeneous deformation. The response is measured in the change of the two thermodynamic functions alluded to: the stored resp. Helmholtz free energy and the dissipation resp. entropy production. The main goal is to show that this idea is computationally feasible for identifying the macro-model material parameters.

The outline of this paper is as follows: In Section 2 the problem is defined in an abstract sense

to motivate the explanation of the proposed strategy for its solution in the following discussion. In Section 3 the stochastic upscaling is described employing the Bayesian identification resp. calibration ideas (Pajonk *et al.* 2012, Rosić *et al.* 2012, 2016). The coarse- and fine-scale models used in this paper will be described in Sections 4 and 5, respectively. These theoretical concepts are numerically applied to several illustrative examples of non-linear inelastic behavior in Section 6. Conclusions are stated in Section 7.

## 2. Problem formulation

Let us assume to be given a symbolic mathematical description of the coarse/macro-scale computational model

$$A_c(u_c, \mathbf{q}) = f_c, \quad (1)$$

in which the operator  $A_c$  describes the system under consideration,  $u_c \in \mathcal{U}_c$  stands for the system state living in a vector space  $\mathcal{U}_c$ ,  $\mathbf{q} = [q_1, \dots, q_n]^T$  are parameters to calibrate the model, and  $f_c$  describes the external influences: the loading, action, initial conditions or experimental set-up. Note that the description given in Eq. (1) is not necessarily stationary but may also cover time-evolution problems. Additionally, the set of parameters  $\mathbf{q}$  may depend on the state  $u_c$  or parts of it as well as on the initial conditions in case of a time-evolution problem.

On the other hand, the same physical phenomena can be modelled quite differently when considered on the fine-scale (detail) level. In an abstract form the corresponding mathematical model reads

$$A_f(u_f) = f_f, \quad (2)$$

in which  $A_f$  stands for the linear or non-linear operator describing discrete or continuum possibly time dependent model,  $u_f \in \mathcal{U}_f$  is the corresponding state and  $f_f$  is the loading program identical to  $f_c$ .

Hence, in order to realistically describe physical phenomena, additional information outlining the finer resolution of the problem in Eq. (2) has to be incorporated into Eq. (1). To achieve this, one has to evaluate at possibly very high cost the response of the fine-scale model and to infer parameters  $\mathbf{q}$  in Eq. (1) in such a way that the predictions of Eq. (1) match those of Eq. (2) as accurately as possible. However, as the two scales do not match with each other ( $\mathcal{U}_c \neq \mathcal{U}_f$ ), the states  $u_c$  and  $u_f$  cannot be directly compared. Instead, the two models are to be compared by some observables or measurements

$$z = y_c + \epsilon = Y_c(\mathbf{q}, u_c(\mathbf{q}, f_c)) + \epsilon, \quad (3)$$

$$y_f = Y_f(u_f(f_f)), \quad (4)$$

on the coarse and fine scale, respectively. The goal of calibration is now to estimate  $\mathbf{q}$  such that  $y_c$  and  $y_f$ , resp.  $z$  and  $y_f$  deviate as little as possible up to the error  $\epsilon$  depicting the discrepancy between the coarse- and fine-scale models.

### 3. Bayesian stochastic upscaling

The set of parameters is not known, and is to be estimated given observable  $z$  and  $y|z$

The deterministic fit is not easy as in general the mapping  $\mathbf{q} \mapsto Y_c(\mathbf{q})$  is not invertible, i.e.,  $z$  does not contain information to uniquely determine  $\mathbf{q}$ , or there are more than one instances of  $\mathbf{q}$  that give a good fit. Therefore, the corresponding ill-posed problem has to be regularized. In a Bayesian view, see e.g., Tarantola (2005), the unknown resp. uncertain parameter of  $\mathbf{q}$  is modelled as a random variable (RV) following the so-called prior distribution taking into account the modeler's limited knowledge. The prior information is seen as a regularization term and is to be corrected to the posterior one by gathering the measurement data. The Bayes theorem is then acting as a decision rule in modelling of  $\mathbf{q}$ , i.e., if the measurement data are to be trusted more or the prior information.

Since the parameters of the model to be estimated are uncertain, all relevant information may be obtained via their stochastic description. Formally, the set of parameters is defined as mapping

$$\mathbf{q} : \Omega \rightarrow \mathbb{R}^n \text{ RVs on a probability space } (\Omega, \mathfrak{A}, \mathbb{P}) \quad (5)$$

in which  $\Omega$  is the set of elementary events,  $\mathfrak{A}$  is a  $\sigma$ -algebra of measurable events, and  $\mathbb{P}$  is a probability measure. The *expectation* corresponding to  $\mathbb{P}$  is denoted by  $\mathbb{E}(\cdot)$ , e.g., the expected value of  $\mathbf{q}$  is given by:  $\bar{\mathbf{q}} := \mathbb{E}(\mathbf{q}) := \int_{\Omega} \mathbf{q}(\omega) \mathbb{P}(d\omega)$ . With  $\mathbf{q}$  formally RVs, the state  $u_c$ , and also the prediction of the "true" measurement  $y_c$  in Eq. (3) are also RVs. Finally, by assuming that the error  $\epsilon(\omega)$  is a RV, then the total prediction of the observation or measurement in Eq. (3)  $z(\omega) = y_c(\omega) + \epsilon(\omega)$  also becomes a RV. In other words, one deals with the *probabilistic* model of the observation, i.e., prediction or *forecast* of the measurement.

#### 3.1 The theorem of Bayes and conditional expectation

Once the fine-scale measurement data are available, the prior information can be updated via Bayes' theorem as formulated by Laplace, commonly accepted as a consistent way to incorporate new knowledge into a probabilistic description (Tarantola 2005). The elementary textbook statement of the theorem is

$$\mathbb{P}(\mathcal{J}_q | \mathcal{M}_z) = \frac{\mathbb{P}(\mathcal{M}_z | \mathcal{J}_q)}{\mathbb{P}(\mathcal{M}_z)} \mathbb{P}(\mathcal{J}_q), \text{ if } \mathbb{P}(\mathcal{M}_z) > 0 \quad (6)$$

in which  $\mathcal{J}_q$  is some subset of possible  $\mathbf{q}$  on which one would like to gain some information, and  $\mathcal{M}_z$  is the new information of non-vanishing measure provided by the measurement. The term depicts  $\mathbb{P}(\mathcal{J}_q)$  *prior*, i.e. the expert's knowledge before the observation  $\mathcal{M}_z$  is made, whereas the quantity  $\mathbb{P}(\mathcal{M}_z | \mathcal{J}_q)$  stands for *likelihood*, the conditional probability of  $\mathbb{P}(\mathcal{M}_z | \mathcal{J}_q)$  assuming that  $\mathcal{J}_q$  is given. Finally, the term  $\mathbb{P}(\mathcal{M}_z)$  is the so-called *evidence*, the probability of observing  $\mathcal{M}_z$  in the first place.

Instead of dealing with the conditional probabilities as in Eq. (6), one may look at the more fundamental notion of *Kolmogorov's conditional expectation* from which conditional probabilities may easily be recovered. The conditional expectation is defined w.r.t sub- $\sigma$ -algebras  $\mathfrak{B} \subset \mathfrak{A}$  of the underlying  $\sigma$ -algebra  $\mathfrak{A}$ . The  $\sigma$ -algebra may be seen as the collection of subsets of  $\Omega$  on which one can make statements about their probability, or in simpler words, as the collection of subsets on which one can learn something through the observation (Bobrowski 2005). By considering RVs

with *finite variance*, i.e., restricted to the Hilbert-space

$$\mathcal{S} := L_2(\Omega, \mathfrak{A}, \mathbb{P}) := \{r : \Omega \rightarrow \mathbb{R} : r \text{ measurable w.r.t. } \mathfrak{A}, \mathbb{E}(|r|^2) < \infty\}.$$

one may define  $\mathfrak{B} \subset \mathfrak{A}$  as sub- $\sigma$ -algebra such that

$$\mathcal{S}_{\mathfrak{B}} := L_2\text{space}(\Omega, \mathfrak{B}, \mathbb{P}) := \{r \in \mathcal{S} : r \text{ measurable w.r.t } \mathfrak{B}\}$$

holds. With  $\mathcal{S}_{\mathfrak{B}}$  being a *closed* subspace, there exists a well-defined continuous orthogonal projection  $P_{\mathfrak{B}} : \mathcal{S} \rightarrow \mathcal{S}_{\mathfrak{B}}$  such that the *conditional expectation* of a RV  $r \in \mathcal{S}$  w.r.t. a sub- $\sigma$ -algebra  $\mathfrak{B}$  reads

$$\mathbb{E}(r|\mathfrak{B}) := P_{\mathfrak{B}}(r) \in \mathcal{S}_{\mathfrak{B}} \quad (7)$$

Being an orthogonal projection, the conditional expectation can be obtained by minimizing the square of error

$$\mathbb{E}(|r - \mathbb{E}(r|\mathfrak{B})|^2) = \min \{\mathbb{E}(|r - \tilde{r}|^2) : \tilde{r} \in \mathcal{S}_{\mathfrak{B}}\}, \quad (8)$$

leading to the *variational equation* or orthogonality relation

$$\forall \tilde{r} \in \mathcal{S}_{\mathfrak{B}} : \mathbb{E}(\tilde{r}(r - \mathbb{E}(r|\mathfrak{B}))) = 0. \quad (9)$$

In our case of an observation of a RV  $z$ , the sub- $\sigma$ -algebra  $\mathfrak{B}$  is the one generated by the *observation*  $z$ , i.e.  $\mathfrak{B} = \sigma(z)$ , and the corresponding conditional expectation is simply denoted as  $\mathbb{E}(r|z) := \mathbb{E}(r|\sigma(z))$ . According to the *Doob-Dynkin* lemma (Bobrowski 2005),  $\mathcal{S}_{\sigma(z)}$  is given by functions of the observation

$$\mathcal{S}_{\sigma(z)} := \{r \in \mathcal{S} : r(\omega) = \phi(z(\omega)), \quad \phi \text{ measurable}\} \quad (10)$$

This means intuitively that anything we learn from an observation is a function of the observation, and the subspace  $\mathcal{S}_{\sigma(z)} \subset \mathcal{S}$  is where the information from the measurement lies. Therefore, following Eq. (7) a RV  $r$  may be decomposed into its orthogonal components w.r.t.  $\mathcal{S}_{\sigma(z)}$  by using

$$\begin{aligned} r &= P_{\sigma(z)}(r) + (I_{\mathcal{S}} - P_{\sigma(z)})(r) \\ &= P_{\sigma(z)}(r) + (I_{\mathcal{S}}r - P_{\sigma(z)}(r)) = \mathbb{E}(r|z) + (r - \mathbb{E}(r|z)), \end{aligned} \quad (11)$$

in which  $(I_{\mathcal{S}} - P_{\sigma(z)})(r) \in \mathcal{S}_{\sigma(z)}^{\perp}$ , the orthogonal complement of  $\mathcal{S}_{\sigma(z)}$ . Obviously,  $P_{\sigma(z)}(r)$  is the best estimator for  $r$  measured in the error norm squared  $\|r - P_{\sigma(z)}(r)\|_{\mathcal{S}}^2$  from the subspace  $\mathcal{S}_{\sigma(z)}$ .

The orthogonal decomposition in Eq. (11) allows the construction of an identification filter by knowing that from a measurement  $z$  one learns something about the component  $P_{\sigma(z)}(r)$  in  $\mathcal{S}_{\sigma(z)}$ . Hence, one simple approach is the least-square approximation, which also underlies the Gauss-Markov theorem and its extensions (Luenberger 1969). If  $\mathbf{q}_p$  is our prior knowledge before the measurement, or the forecast, one thus defines the filtered, analyzed, or assimilated RV  $\mathbf{q}_a$  having the observation  $\check{y}$  from Eq. (11) as

$$\begin{aligned} \mathbf{q}_a &= \mathbb{E}(\mathbf{q}_p|\check{y}) + (\mathbf{q}_p - \mathbb{E}(\mathbf{q}_p|z)) \\ &= \mathbf{q}_p + (\mathbb{E}(\mathbf{q}_p|\check{y}) - \mathbb{E}(\mathbf{q}_p|z)) = \mathbf{q}_p + \mathbf{q}_i \end{aligned} \quad (12)$$

in which  $\mathbf{q}_i = \mathbb{E}(\mathbf{q}_p|\check{y}) - \mathbb{E}(\mathbf{q}_p|z)$  is called the *innovation*, and as  $\mathbb{E}(\mathbf{q}_a|\check{y}) = \mathbb{E}(\mathbf{q}_p|\check{y})$ , it follows, that  $\mathbb{E}(\mathbf{q}_i|\check{y}) = 0$ . Eq. (12) is the *nonlinear* conditional expectation-filter (Matthies *et al.* 2016), but as  $\mathbb{E}(\mathbf{q}_p|z)$  can be a complicated function of  $z$ , it may be difficult to compute. A simpler version results if in Eq. (10) one takes only the affine functions, i.e., a smaller subspace

$$\mathcal{S}_{\sigma(z),1} := \{r \in \mathcal{S} : r(\omega) = H(z(\omega)) + b, \quad H \text{ linear}\} \subset \mathcal{S} \quad (13)$$

and the minimization Eq. (8) is performed over this smaller subspace, resulting in an optimal linear map  $\mathbf{K}_q$  (the so-called Kalman-gain) (Matthies *et al.* 2016, Luenberger 1969). With this simplification in Eq. (12) one arrives at the *Gauss-Markov-Kalman-filter* (GMKF)

$$\begin{aligned} \mathbf{q}_a &= \mathbf{q}_p + (\mathbf{K}_q(\check{y}) - \mathbf{K}_q(z)) \\ &= \mathbf{q}_p + \mathbf{K}_q(\check{y} - z) = \mathbf{q}_p + \mathbf{K}_q(\check{y} - (Y_c(\mathbf{q}_p) + \epsilon)) \end{aligned} \quad (14)$$

given in terms of RVs  $\mathbf{q}_p(\omega)$  and  $z(\omega)$ , which for computational purposes have to be discretized.

### 3.2 Spectral or functional approximation

Having that Eq. (14) is a relation between RVs, it certainly also holds for samples of the RVs, and this is the basis of the ensemble Kalman filter, the EnKF (Evensen 2009). The sampling points are sometimes also denoted as particles, and the EnKF is a simple version of a particle filter. However, here we want to pursue the more promising functional or spectral approximation (Matthies *et al.* 2016, Matthies 2007) for all the RVs in Eq. (14). This means that all RVs, say  $\mathbf{q}(\omega)$ , are described as functions of known RVs  $\{\theta_1(\omega), \dots, \theta_l(\omega), \dots\}$ . Often, when for example stochastic processes or random fields are involved, one has to deal here with infinitely many RVs, which for an actual computation have to be truncated to a finite number of significant RVs stored in a vector  $\boldsymbol{\theta}(\omega) = [\theta_1(\omega), \dots, \theta_n(\omega)]$ . We shall assume that these have been chosen as Gaussian and uncorrelated, thus they can be considered as independent. This allows a choice of a finite set of linearly independent functions  $\{\Psi_\alpha\}_{\alpha \in \mathcal{J}_M}$  of the variables  $\boldsymbol{\theta}(\omega)$ , where the index  $\alpha$  is a multi-index, and the set  $\mathcal{J}_M$  is a finite set of multi-indices with cardinality (size)  $M$ . Among different systems of functions that can be used, here the classical choice of multivariate polynomials is made - leading to the *polynomial chaos expansion* (PCE) (Matthies 2007). Thus, a RV  $\mathbf{q}(\omega)$  is replaced by a functional approximation

$$\hat{\mathbf{q}}(\omega) = \sum_{\alpha \in \mathcal{J}_M} \mathbf{q}_\alpha \Psi_\alpha(\boldsymbol{\theta}(\omega)) = \sum_{\alpha \in \mathcal{J}_M} \mathbf{q}_\alpha \Psi_\alpha(\boldsymbol{\theta}) = \hat{\mathbf{q}}(\boldsymbol{\theta}) \quad (15)$$

The argument  $\omega$  will be omitted from here on, as the probability measure  $\mathbb{P}$  on  $\Omega$  is transported to  $\boldsymbol{\Theta} = \Theta_1 \times \dots \times \Theta_n$ , the range of  $\boldsymbol{\theta}$ , giving  $\mathbb{P}_\theta = \mathbb{P}_1 \times \dots \times \mathbb{P}_n$  as a product measure, in which  $\mathbb{P}_l = (\theta_l) * \mathbb{P}$  is the distribution measure of the RV  $\theta_l$ , as the RVs  $\theta_l$  are independent. All computations following this stage are performed on  $\boldsymbol{\Theta}$ , typically some subset of  $\mathbb{R}^n$ . Hence,  $n$  is the dimension of the problem, and if  $n$  is large, one faces a high-dimensional problem. The filter Eq. (14) then reads (see Matthies *et al.* (2016) for more details)

$$\hat{\mathbf{q}}_a(\boldsymbol{\theta}) = \hat{\mathbf{q}}_p(\boldsymbol{\theta}) + \mathbf{C}_{\hat{\mathbf{q}}_p \hat{z}} \mathbf{C}_{\hat{z}}^{-1}(\check{y} - \hat{z}(\boldsymbol{\theta})) = \hat{\mathbf{q}}_p(\boldsymbol{\theta}) + \mathbf{K}_{\hat{q}}(\check{y} - \hat{z}(\boldsymbol{\theta})) \quad (16)$$

If the approximating functions are polynomials, the last expression is known as a *spectral*

*Kalman filter* (SPKF). Inserting the functional approximations into Eq. (16), one obtains an explicit and easy to evaluate expression for the assimilated or updated variable in terms of the input.

#### 4. The coarse-scale model

For simplicity reasons the continuum model on the coarse scale in Eq. (1) in Section 2 is assumed to be of standard generalized type (Halpen and Nguyen 1974, Halpen and Nguyen 1975, Nguyen 1977) characterized by infinitesimal displacements/strains and spatially constant material properties. In particular here are considered the pressure sensitive materials such as concrete and rocks described in a simplified manner using the Drucker-Prager yield criterion for plastic and damage criterion based on a spherical part of the stress tensor in compression as proposed in Ibrahimbegović (2009). The behavior of such materials is completely characterized by two functions: the stored resp. Helmholtz free energy density  $\psi_c(\boldsymbol{\varepsilon}, \mathbf{w}, \mathbf{q})$  for the reversible part, and the dissipation pseudo-potential density  $\varphi_c(\dot{\boldsymbol{\varepsilon}}, \boldsymbol{\varepsilon}, \mathbf{w}, \dot{\mathbf{w}}, \mathbf{q})$  for the irreversible part, and the assumption of maximal dissipation. Here,  $\boldsymbol{\varepsilon}$  is the strain,  $\mathbf{w}$  is a collection of internal phenomenological variables (the memory of the material), and  $\mathbf{q}$  is a collection of parameters specifying the detailed character of the functions  $\psi_c$  and  $\varphi_c$ .

##### 4.1 Constitutive equations

The constitutive description of the coarse-scale material is assumed to follow an associated rate-independent law with linear hardening described by the Helmholtz free energy

$$\psi_c(x, \boldsymbol{\varepsilon}, \mathbf{w}, \mathbf{q}) = \underbrace{\frac{1}{2} \boldsymbol{\varepsilon}_e \mathbf{C} \boldsymbol{\varepsilon}_e}_{\psi_e} + \underbrace{\frac{1}{2} \sigma D \sigma}_{\psi_d} + \frac{1}{2} K_p v_p^2 + \frac{1}{2} K_d v_d^2 \quad (17)$$

in which the vector  $\mathbf{w}$  contains the plastic  $\{\boldsymbol{\varepsilon}_p, v_p\}$  and damage  $\{\boldsymbol{\varepsilon}_d, v_d\}$  internal variables, whereas the parameter  $\mathbf{q}$  consists of the isotropic and homogeneous elastic constitutive tensor  $\mathbf{C}$  given as a function of bulk  $\kappa$  and shear  $G$  moduli, the plastic  $K_p$  and damage  $K_d$  isotropic hardening coefficients, and the damage compliance tensor  $D$  relating damage strain  $\boldsymbol{\varepsilon}_d$  and  $\sigma$ . Moreover, the dissipation functional is given by

$$\varphi_c(x, \dot{\boldsymbol{\varepsilon}}, \boldsymbol{\varepsilon}, \mathbf{w}, \dot{\mathbf{w}}, \mathbf{q}) = \underbrace{(\boldsymbol{\sigma} \cdot \dot{\boldsymbol{\varepsilon}}_p + \chi_p \dot{v}_p)}_{\varphi_c^p} + \underbrace{\left(\frac{1}{2} \boldsymbol{\sigma} \cdot D \boldsymbol{\sigma} + \chi_d \dot{v}_d\right)}_{\varphi_c^d} \quad (18)$$

in which  $\chi_p$  and  $\chi_d$  are the plastic and damage hardening forces related to the respective strain-like hardening variables  $v_p$  and  $v_d$ . Finally, the evolution is driven by the prescribed admissible stress domain represented by plastic and damage yield functions

$$f_p(\boldsymbol{\sigma}, \chi_p) = \sqrt{\text{dev}(\boldsymbol{\sigma}) : \text{dev}(\boldsymbol{\sigma})} - \frac{1}{3} \text{tr}(\boldsymbol{\sigma}) \tan(\alpha) - \sqrt{\frac{2}{3}} (c - \chi_p), \quad (19)$$

$$f_d(\sigma, \chi_d) = \langle -\text{tr}(\sigma) \rangle - (\sigma_f - \chi_d), \quad (20)$$

respectively. Here, Eq. (19) describes the Drucker-Prager yield function for plasticity, in which  $c$  denotes the cohesion and  $\alpha$  is the friction angle here modelled via the parameter  $c_\alpha = \frac{c}{\tan(\alpha)}$ . Similarly, Eq. (20) represents the damage yield function in which  $\sigma_f$  signifies the failure stress. By gathering all model parameters into one vector we have

$$\mathbf{q} = [\log \kappa, \log G, \log c, \log K_p, \log c_\alpha, \log \sigma_f, \log K_d], \quad (21)$$

The goal is to infer  $\mathbf{q}$  given the fine scale measurement data and their coarse-scale prediction as described in Eq. (3). The latter one is formulated in a more concrete form

$$Y_c(\mathbf{q}) = \left[ \int \psi_c(x, \varepsilon, \mathbf{w}, \mathbf{q}) dV, \int \varphi_c(x, \varepsilon, \dot{\varepsilon}, \mathbf{w}, \dot{\mathbf{w}}, \mathbf{q}) dV \right] \quad (22)$$

as the spatial averages of the stored and dissipated energies in the domain - one quadrilateral element of the coarse-scale model.

#### 4.2 Variational formulation

For the sake of completeness with regards to the material description, in this section we briefly dwell on the details of the numerical implementation of the constitutive model under consideration following Markovic and Ibrahimbegović (2006). By taking the displacement and stress variables as unknown state, the mixed weak formulation of the problem is obtained from the Hellinger-Reissner principle given below.

$$\Pi_{comp}(u, \sigma) = \int_G (-\phi_c^e(\sigma) - \phi_c^d(\sigma, D) + \sigma(\nabla u - \varepsilon^p)) dV - \int_{\Gamma_\sigma} u \cdot t dA \quad (23)$$

where  $\phi_c^e(\sigma)$  and  $\phi_c^d(\sigma, D)$  are the complementary energy densities. By enforcing the stationary condition on Eq. (23) with respect to the variation of the states  $\sigma$  and  $u$  we get

$$\delta \Pi_{comp} = \frac{\partial \Pi_{comp}}{\partial u} \delta u + \frac{\partial \Pi_{comp}}{\partial \sigma} \delta \sigma = 0, \quad \forall \delta u, \delta \sigma. \quad (24)$$

from which the equilibrium equation and the additive decomposition of the strain read

$$\int_G \nabla^s \delta u dV - \int_{\Gamma_\sigma} \delta u \cdot t dA = 0, \quad \forall \delta u, \quad (25)$$

$$\int_G [\nabla^s - \varepsilon^p - \mathcal{D}\sigma - \mathcal{C}^{-1}\sigma] dV = 0, \quad \forall \delta \sigma. \quad (26)$$

Note that this formulation directly leads to the hypothesis of the additive decomposition of strain, which is usually assumed a priori in the strain-based approach (Ibrahimbegović *et al.* (2003). Regarding the spatial discretisation of Eq. (25) to Eq. (26), both displacement and stress fields are discretised in the finite element setting as proposed in Pian and Sumihara (1984).

In the deterministic setting the last two equations would represent the full discretisation of the problem given in Eqs. (25) to (26). The estimation of the state in time sequence  $\{t_n\}$  follows the

computational algorithm consisting of three stages: global, elemental and the local (integration point) one. On the global or node level, the discretised equilibrium in Eq. (25) (i.e., the non-linear residual equation) is solved by a Newton-like procedure for the increment of displacement  $\Delta u_n$ . On the element level, the stress interpolation parameters are determined by solving the discrete form of Eq. (26). The internal variables associated with damage/plasticity are evaluated using the closest point projection scheme at the Gauss integration points.

Finally, we would like to remark that the stress-based approach is computationally more efficient than the strain-based counterpart, because it does not need an additional iterative loop to enforce equivalence of computed stress, required in the latter approach (Ibrahimbegović *et al.* 2003).

#### 4.3 Stochastic formulation- forecast

The constitutive model as described in the previous section is deterministic, and is to be extended into its probabilistic counterpart in order to take into account the prior uncertainty of the material properties describing the expert's knowledge as depicted in Section 3. As all the model parameters are positive, one actually models their logarithms, see Eq. (21), which are unconstrained and at the same time producing the proper metric. This allows  $\mathbf{q}$  to be a priori modelled as a vector of independent normally distributed random variables according to the maximum entropy principle such that the original parameters follow a log-normal distribution as prior.

In the Bayesian identification the uncertain material parameters are random variables, and hence the coarse scale material is a *stochastic* one. In other words, the stored energy  $\psi_c$  and the dissipation  $\varphi_c$  densities in Eqs. (17) and (18) become random variables. Additionally, to their spatial dependence on the location  $x$ , both densities are also formally functions of the variable  $\omega \in \Omega$ , i.e., elementary probability events as described in Section 3. The simulation of the coarse- scale model hence corresponds to the process of solving a stochastic problem which has a similar form to the deterministic one (Ibrahimbegović and Matthies 2012, Matthies and Ibrahimbegović 2014). Computationally, the striking difference upon full discretization lies in the problem dimension. Namely, the state variable lives in a space obtained as the tensor product of the corresponding deterministic space and the space of random variables  $\mathcal{S}$ . Thus, the stochastic problem requires a temporal, spatial, and stochastic discretization, largely increasing the problem dimension and thus the computational effort. For a full discussion of such computations, see (Rosić and Matthies 2014).

In this paper the stochastic discretization is done in a functional approximation setting as already described in Section 3.2, i.e., for both the displacement and stress variables as ansatz are taken the polynomial chaos expansions, the coefficients of which are found by pseudo-spectral projection resp. regression (Rosić and Matthies 2014). Once the solution response is approximated, the prior predictive, i.e., the prediction of the measurement, is evaluated by obtaining the spatial averages of the energy densities

$$Y_c(\hat{\mathbf{q}}) = \left[ \int \psi_c(x, \omega, \hat{\varepsilon}, \hat{\mathbf{w}}, \hat{\mathbf{q}}) dV, \int \varphi_c(x, \omega, \hat{\varepsilon}, \hat{\dot{\varepsilon}}, \hat{\mathbf{w}}, \hat{\mathbf{q}}) dV \right] \quad (27)$$

In contrast to Eq. (22) here the measurements are random variables, which also can be approximated by the polynomial chaos expansions.

## 5. The fine-scale model

To sketch the upscaling procedure, for simplicity reasons the fine-scale or “micro-scale model” is taken to be the fine-discretised version of the coarse-scale continuum model based on the standard generalized theory, see Section 4. However, any other kind of model which allows a “measurement” resp. computation of stored and dissipated energies could be also used.

The discretisation is refined such that the *only one* quadrilateral element on the coarse scale is split into 2500 finer quadrilateral elements. Additionally, the material parameters  $\mathbf{q}$  are assumed to be isotropic and heterogeneous, the spatial dependence of which is modelled by one realization of normally distributed random fields described by isotropic stationary Gaussian correlation functions. Even though described by random fields, the spatially varying  $\mathbf{q}$  is in the bottom line deterministic and unknown to the coarse-scale model in the identification procedure. The information about the parameter value can be only indirectly observed via spatially averaged the fine-scale stored resp. Helmholtz free energy density  $\psi_f(x, \varepsilon_f, \mathbf{w}_f)$  and the fine-scale dissipation pseudo-potential density  $\varphi_f(x, \varepsilon_f, \dot{\varepsilon}_f, \mathbf{w}_f, \dot{\mathbf{w}}_f)$ , i.e.,

$$Y_f = \left[ \int \psi_f(x, \varepsilon_f, \mathbf{w}_f) dV, \int \varphi_f(x, \varepsilon_f, \dot{\varepsilon}_f, \mathbf{w}_f, \dot{\mathbf{w}}_f) dV \right]. \quad (28)$$

Here, the variables  $\varepsilon_f$  and  $\mathbf{w}_f$  as well as their evolution rates have the same physical meaning as in the coarse-scale model given in Section 4.

## 6. Numerical results

To illustrate the proposed strategy, the upscaling is tested on several numerical examples in which the fine-scale configurations are taken in both homogeneous (one realisation of a random variable) and heterogeneous (one realisation of a random field) forms. The former one is of particular importance for the validation purposes, whereas the latter one explores more practical examples with spatially varying material properties. Additionally, different loading cases necessary to trigger the identification of all the relevant material parameters are used. These correspond to the boundary displacements enforced by specifying the respective displacement gradient given as

$$\mathbf{u}_b = \mathbf{H} \mathbf{x}_b, \quad (29)$$

in which  $\mathbf{u}_b$  and  $\mathbf{x}_b$  stand for the boundary displacements and nodal coordinates, respectively. Here, only two modes of the deformation gradient  $\mathbf{H}$  are taken as specified in Table 1. However, these are further linearly combined in various manners such that each combination defines one experiment. Moreover, the update of the coarse-scale parameters is performed in a sequential way such that the energy measurements from the first experiment are used to obtain the intermediate posterior which further serves as a prior for the second experiment, etc.

Table 1 Deformation matrix for different loading cases

$H_I$	$H_{II}$
$\begin{bmatrix} 0.0 & 1.0 \\ 1.0 & 0.0 \end{bmatrix}$	$\begin{bmatrix} 1.0 & 0.0 \\ 0.0 & 1.0 \end{bmatrix}$

### 6.1 The homogeneous case

In order to validate the identification procedure for the non-linear type of measurements such as the energy integrals in this paper, both the fine- and coarse-scale descriptions are taken as homogeneous ones, and the corresponding variational formulations are discretised by same quadrilateral element. The coarse-scale parameters follow the log-normal distributions, a priori characterized by the second order characteristics, whose mean values have a 10% off-set from their deterministic fine scale counterpart (shown in Table 2) and have 10% coefficient of variation.

Table 2 Fine scale truth and coarse scale prior statistics (in MPa)

Property	$\kappa$	$G$	$c$	$K_p$	$c_\alpha$	$\sigma_f$	$K_d$
Fine truth	204000	92000	300	450	500	300	450

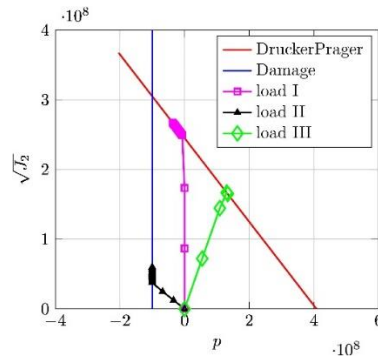


Fig. 1 Load evolution on coarse scale to update material parameter using homogeneous fine-scale measurements

The upscaling is considered for elastic, plastic or damage parameters separately, i.e., for the given loading case, the parameters other than those being identified, are kept known and deterministic. To trigger different dissipation mechanisms under consideration, several loading histories are constructed as shown in Fig. 1. As results we show the percentile estimates of the updated parameters.

We first consider the update of elastic parameters for which the first two steps of Load I followed by the first two steps of Load III (see Fig. 1) are used. As apparent from Fig. 2(a)-(b), the coarse-scale elastic parameters are updated quite well with the posterior distribution pivoted about the fine-scale truth and the prior uncertainty significantly reduced. Having that the first two loading steps characterize shear deformation, one may note that in the beginning only  $G$  is updated, whereas the information on  $\kappa$  is contained in the energy measurements from the third step onwards. From this fine-scale measurement the posterior mean value shifts in the proximity of true one and the variance reduces. This is expected as the third and fourth load steps of Load III impart predominantly volumetric deformation characterizing  $\kappa$ . In order to illustrate the effect of loading on the identification, the same numerical setup as before is considered only with loading sequence being reversed i.e. the first two steps of Load III followed by the first two steps of Load I are applied. In this case, as expected,  $\kappa$  is identified before  $G$ , see Fig. 3.

For the plastic parameters shown in Fig. 4(a)-(c) with Load I considered for the identification process, the prior distributions describing  $c$  and  $K_p$  are updated significantly around step 4-6, indicating that the plastic deformation has kicked in, and the posterior converges uniformly to the true value in the subsequent steps. One thing to note is that it takes fewer steps for  $c$  to update than  $K_p$ . On the other hand, the update of  $c_\alpha$  seems less satisfactory as the mean converges to the true value around the sixth loading step.

Finally, the update of the damage parameters is shown in Fig. 5(a)-(b) with the compression Load II used for the identification procedure. The mean of posteriors describing  $\sigma_f$  and  $K_d$  converges to the true value around points 4 and 10, respectively. Moreover, the mean of  $\sigma_f$  shifts in fewer steps to the true value as compared to  $K_d$  which is akin to the trend observed in the update of plastic parameters. This is understandable behaviour as the update of cohesion or fracture stress (for plastic and damage case respectively) requires just the inception of plastic and damage phenomena as information. However, the hardening parameters need significant changes in material hardening in order to have sufficient information for update.

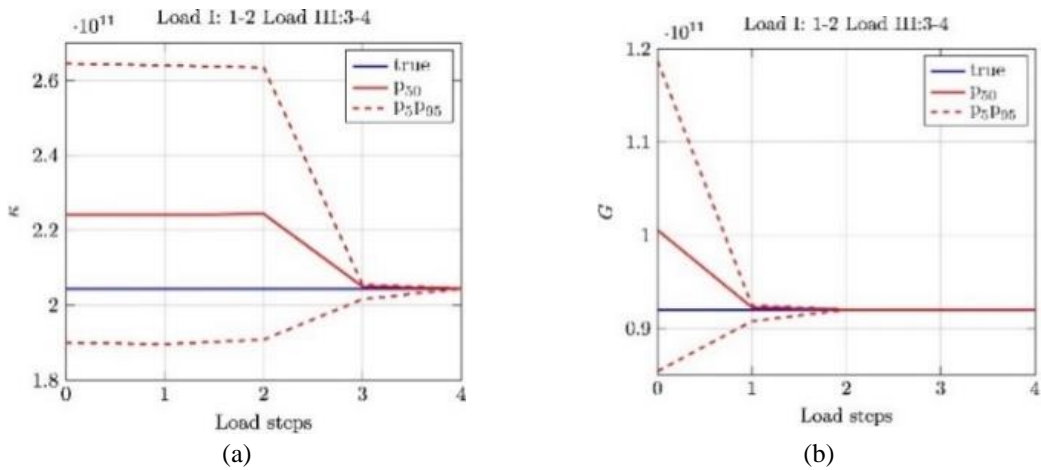


Fig. 2 Updated elastic material parameters using homogeneous fine-scale measurements

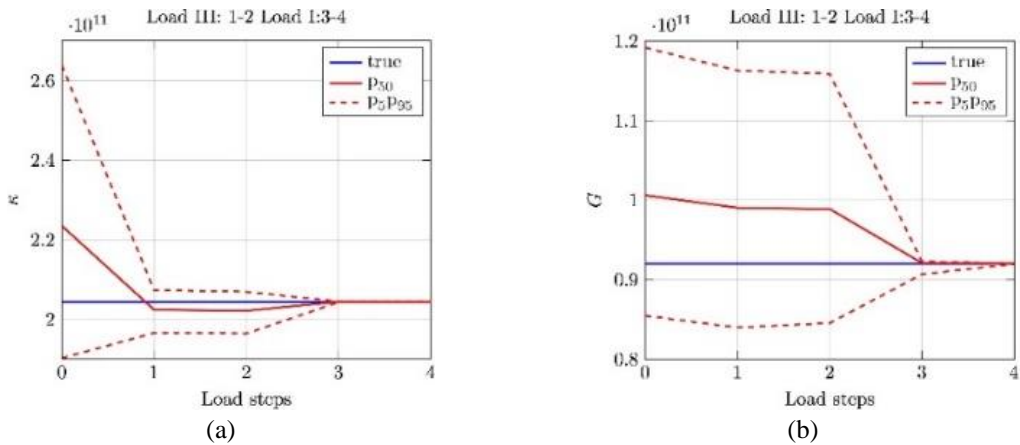


Fig. 3 Updated elastic material parameters using homogeneous fine-scale measurements with loading sequence reversed

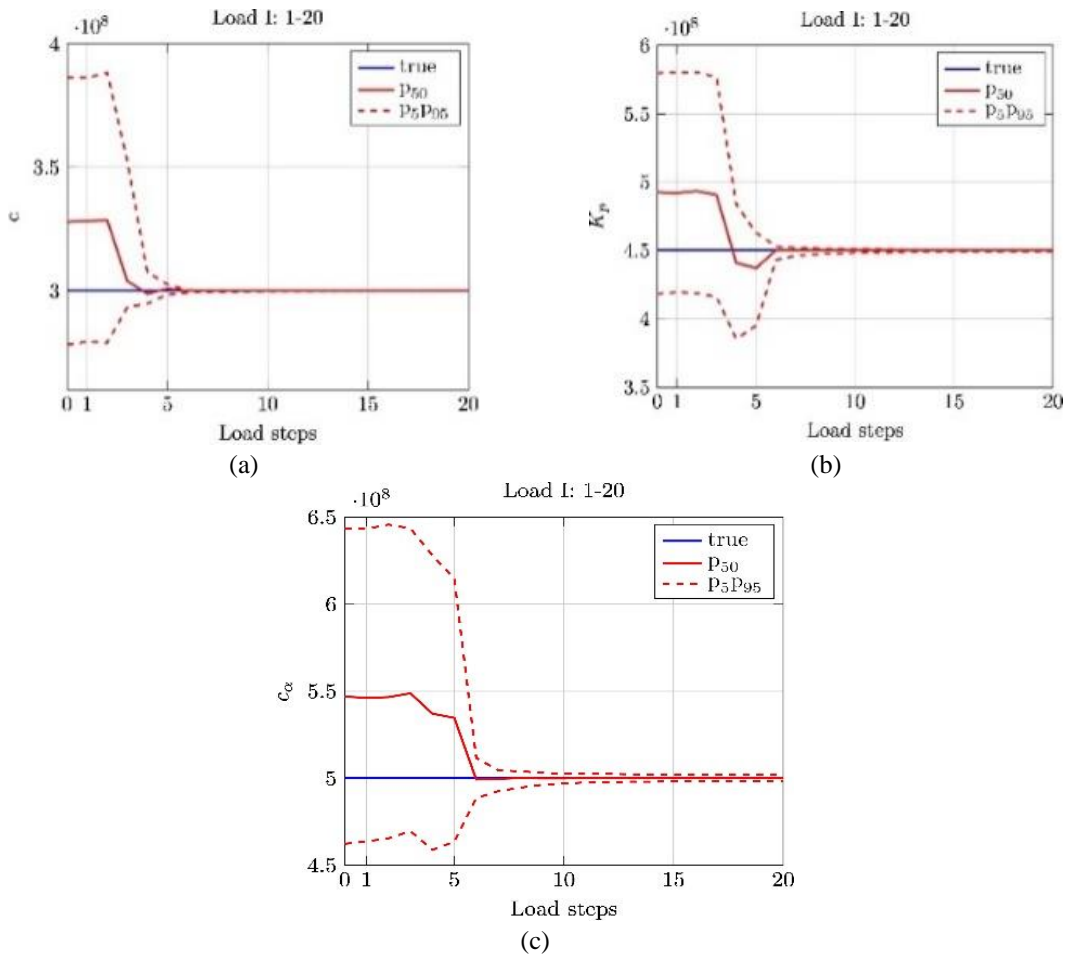


Fig. 4 Updated plastic material parameters using homogeneous fine-scale measurements

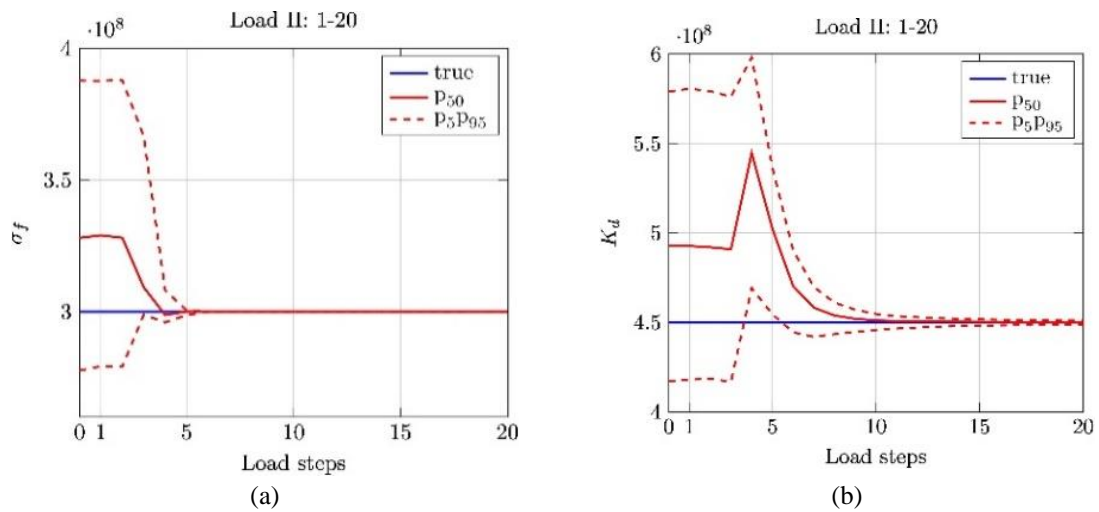


Fig. 5 Updated damage material parameters using homogeneous fine-scale measurements

## 6.2 The heterogeneous case

We now turn our attention to the more realistic case in which the material properties on the fine scale are assumed to be spatially varying. In this scenario, the fine scale is discretised using 2500 elements, the spatial variability of elastic  $\{\kappa, G\}$ , plastic  $\{c, K_p, c_\alpha\}$  and damage  $\{\sigma_f, K_d\}$  parameters is realized by taking them as a realization of a log - normal random field with second order characteristics. To generate the realizations, the mean value of parameters are taken same as the “Fine truth” for the homogeneous case (shown in Table. 1). The coefficient of variation is taken as 5% and the correlation length is 10 times the characteristic length of the fine-scale element with a Gaussian covariance function. The upscaling is performed for each phenomenon separately meaning that on the coarse scale the parameters other than those being updated are kept deterministic. Moreover, two updating approaches are considered:

- *Sequential*: The parameters are updated sequentially i.e., the information from fine scale is added at each load step and the current posterior is taken as a new prior for the next update.
- *Smoothing*: The whole history of measurements is used in one go to update the coarse- scale parameters.

As results, we show the percentiles and updated distributions for the coarse-scale material parameters using the *sequential* and *smoothing* approach respectively. In addition, we also

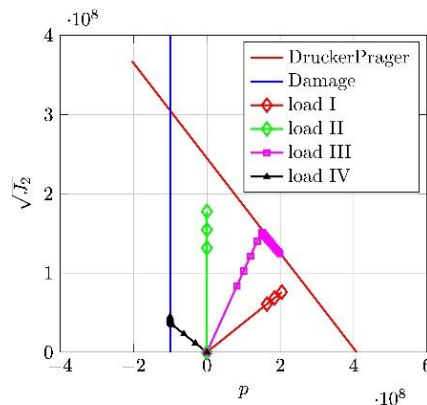


Fig. 6 load evolution on coarse scale to update material parameters using heterogeneous fine-scale measurements

compare the percentiles of different energy measures (used for upscaling) computed from the prior and updated distribution of the coarse-scale values with the corresponding fine-scale ones. In this case, we denote the prior and posterior percentile estimates as  $pr$  and  $pf$  respectively.

### 6.2.1 Update of elastic parameters

For the update of the elastic parameters, the loading consists of three steps from Load I (bi-axial tension, notice that there will be some shear component in this case as we consider plain strain case) followed by three steps from Load II (pure shear). The loading is graphically illustrated in Fig. 6. The loading cases are executed independently i.e., each loading programme

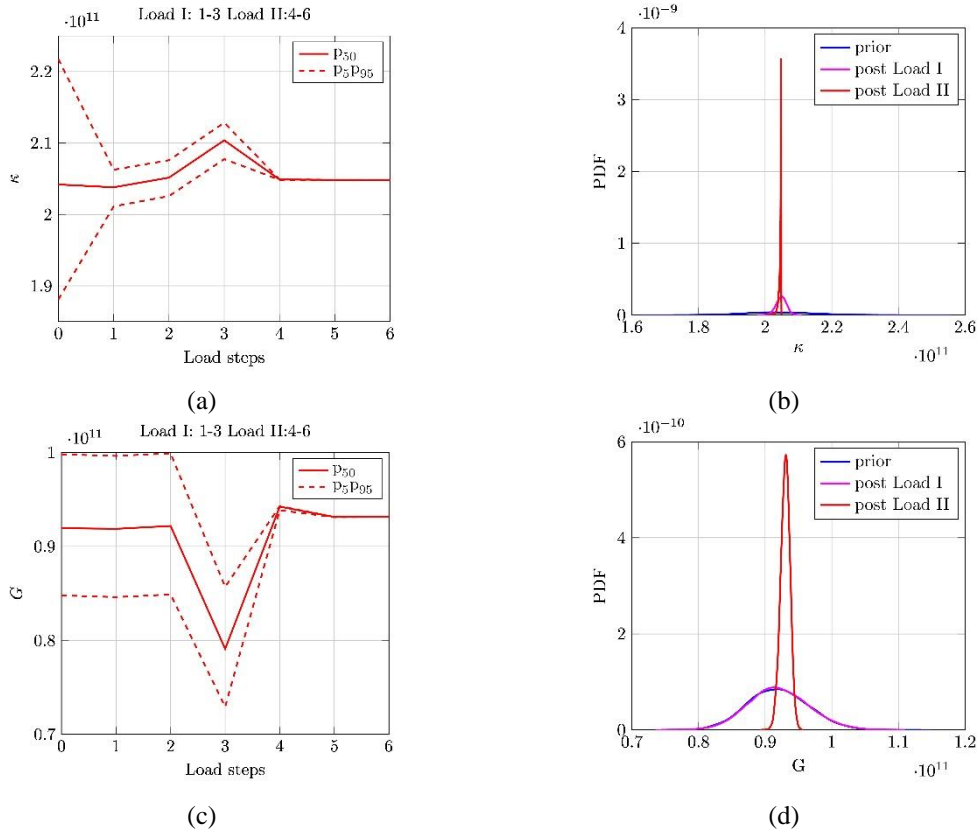


Fig. 7 Updated elastic material parameters using heterogeneous fine-scale measurements from *sequential* (a), (c) and *smoothing* (b), (d) approaches

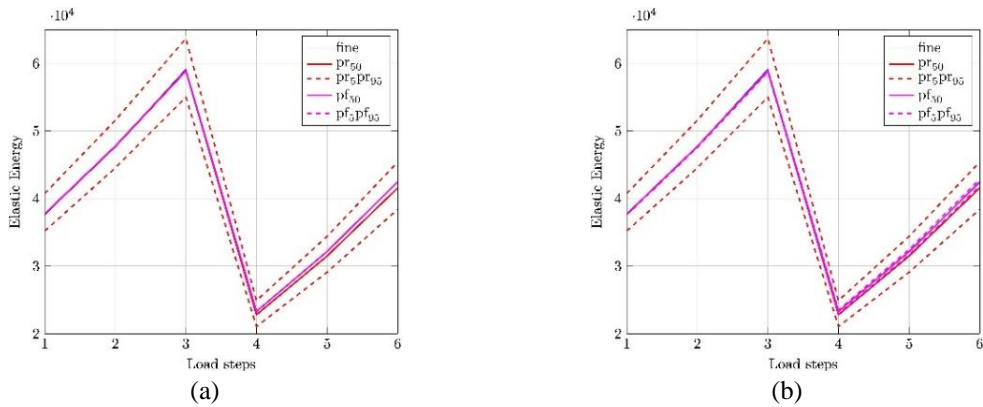


Fig. 8 Comparison of the percentile estimates of energy measures computed from the prior ( $pr_5$ ,  $pr_{50}$  and  $pr_{95}$ ) and the updated ( $pf_5$ ,  $pf_{50}$  and  $pf_{95}$ ) elastic parameters with the fine-scale values using *sequential* (a) and *smoothing* (b) approaches

starts with an undeformed configuration.

The update using the *sequential* approach is shown in Fig. 7(a)-(c). During the first three

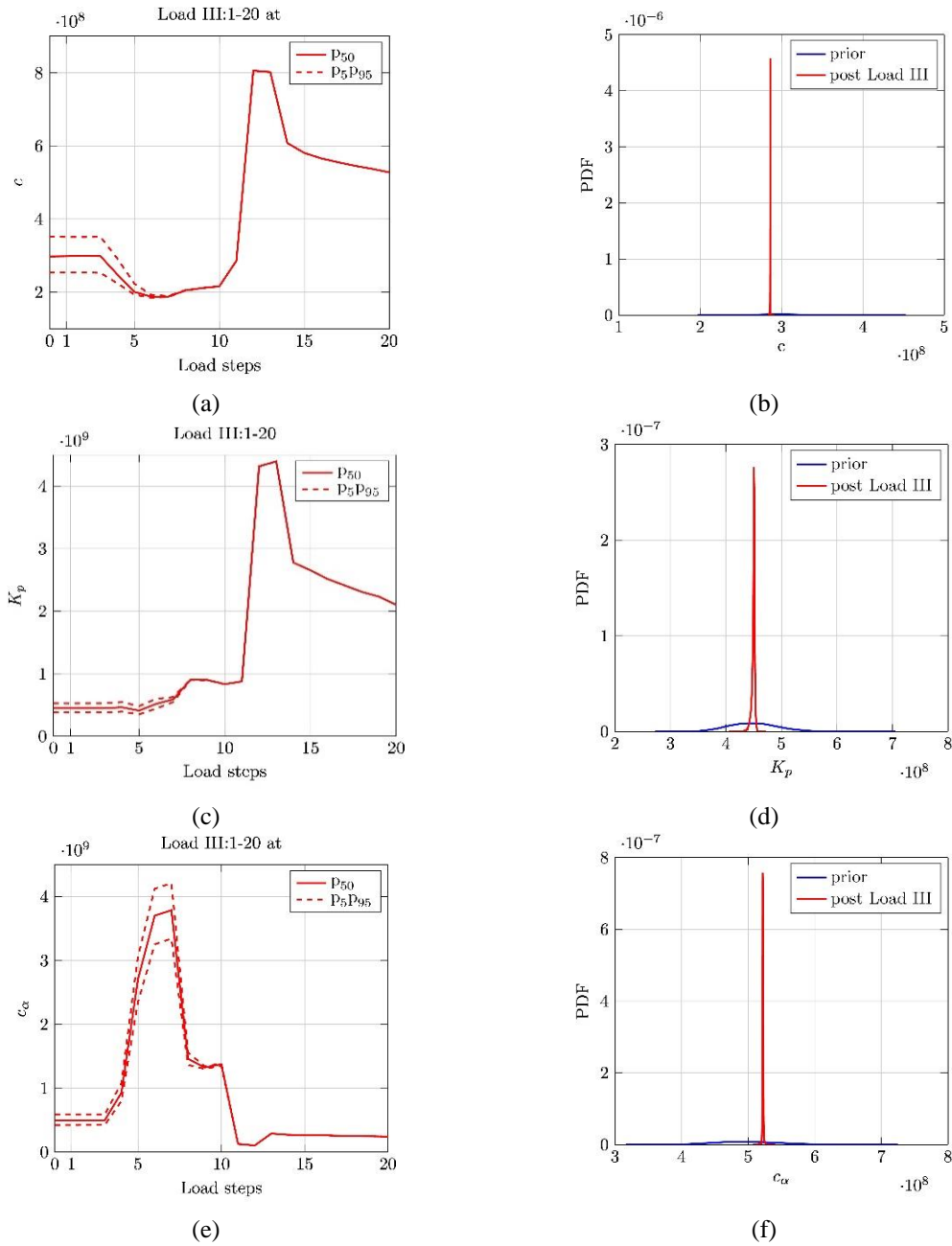


Fig. 9 Updated plastic material parameters using heterogeneous fine-scale measurements from *sequential* (a), (c), (e) and *smoothing* (b), (d), (f) approaches

loading steps the mean of  $\kappa$  starts moving with reduced uncertainty illustrated by  $p_5$  and  $p_{95}$  quantiles. For  $G$ , the reduction in uncertainty becomes noticeable only from 4th step onwards as the load steps are characterised by shear deformation. On the other hand, the update using the whole history is shown in Fig. 7(b)-(d). In this case the whole loading history for the two cases is

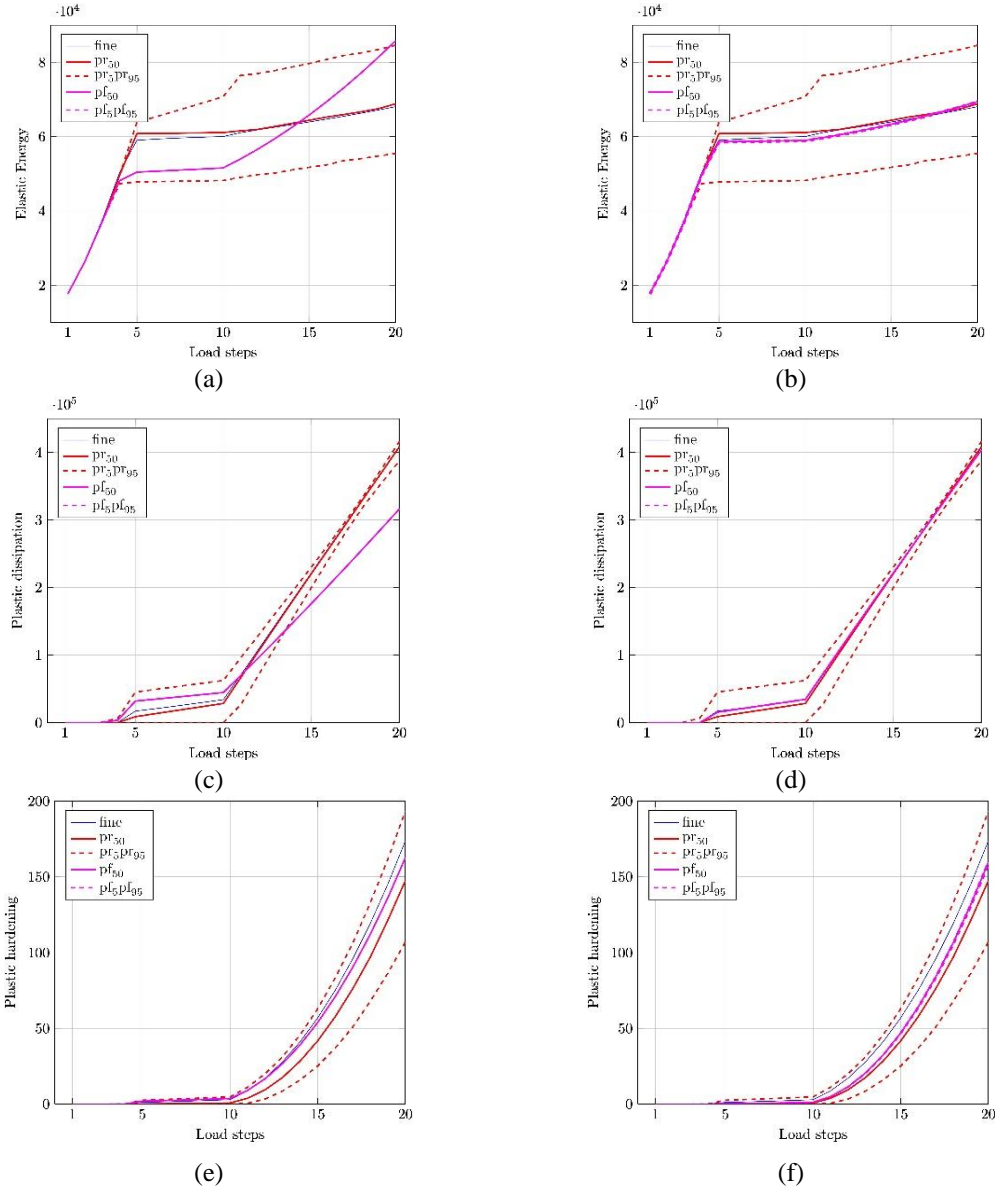


Fig. 10 Comparison of the percentile estimates of energy measures computed from the prior ( $pr_5$ ,  $pr_{50}$  and  $pr_{95}$ ) and the updated ( $pf_5$ ,  $pf_{50}$  and  $pf_{95}$ ) plastic parameters with the fine-scale values using *sequential* (a), (c), (e) and *smoothing* (b), (d), (f) approaches

added sequentially, meaning that the update is performed by concatenating the two loading histories one after the other. Similar to the *sequential* case  $\kappa$  is updated during the first step (i.e., by using measurements from steps 1-3) whereas  $G$  remains oblivious to added information. The shear modulus only updates in the second step (i.e. by using measurements from step 4-6).

In order to check the validity of the update, the posterior predictive of elastic energies, obtained by propagating the posterior  $\kappa$  and  $G$  values through the coarse-scale model under the same

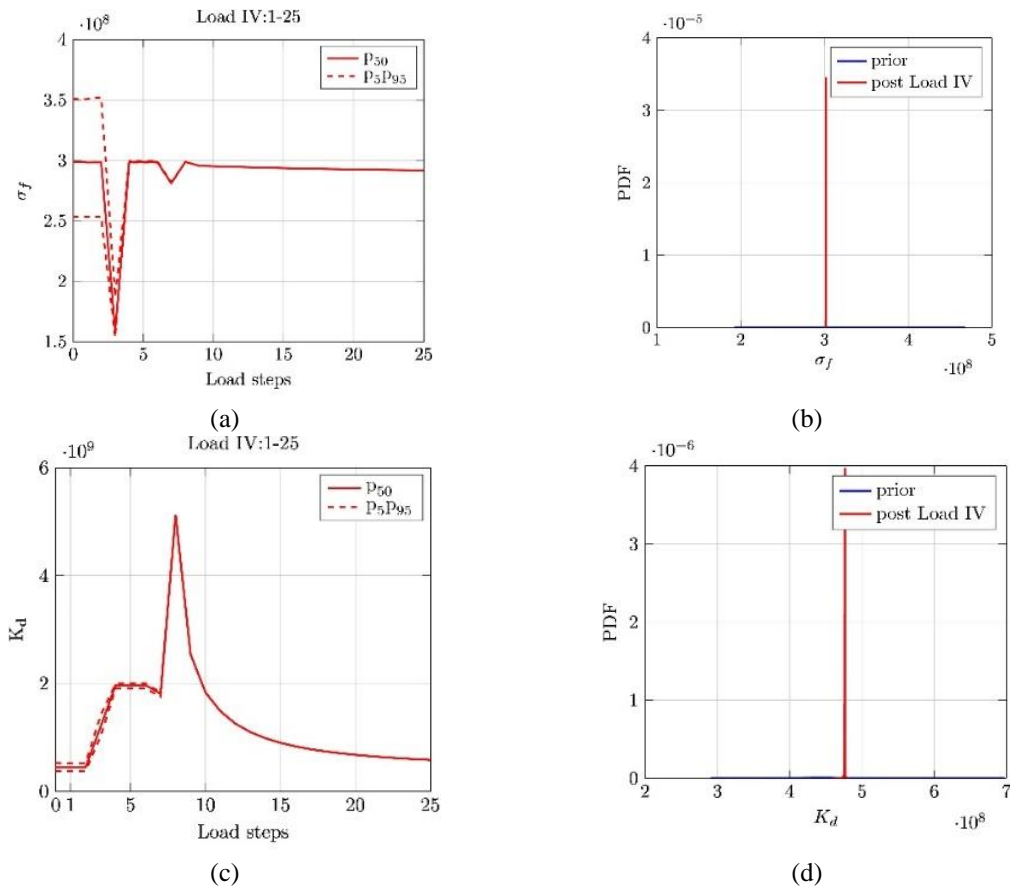


Fig. 11 Updated plastic material parameters using heterogeneous fine-scale measurements from *sequential* (a), (c) and *smoothing* (b), (d) approaches

loading program, are compared to the prior predictive energies and the fine-scale counterpart in Fig. 8(a)-(b). As the posterior 95% interval shrinks to the fine-scale truth for both *sequential* and *smoothing* approaches, one may conclude that the upscaling procedure is successful.

### 6.2.2 Update of plastic parameters

The loading program for the update of plastic parameters is shown as Load III (combination of bi-axial tension and pure shear) in Fig. 6. The load steps are chosen such that one hits the yield surface, and thus extracts the information about the plastic phenomenon. The evolution of *sequential* updates is shown in Fig. 9(a), (c) and (e) in which one could immediately observe that there is no convergence in the mean for  $c$  and  $K_p$ . On the other hand, the mean of  $c_\alpha$  stabilizes after 13 steps. The results for the *smoothing* update are shown in Fig. 9(a), (d) and (f). To validate such an obtained posterior distribution, the posterior predictive energies (the elastic energy, plastic dissipation and stored hardening energy) evaluated in a similar manner as in the elastic case are depicted in Fig. 10. By comparing the respective 95% regions to the fine-scale measurement, one may conclude that the *smoothing* update performs better than the *sequential* one in terms of mimicking the energy response of the fine scale.

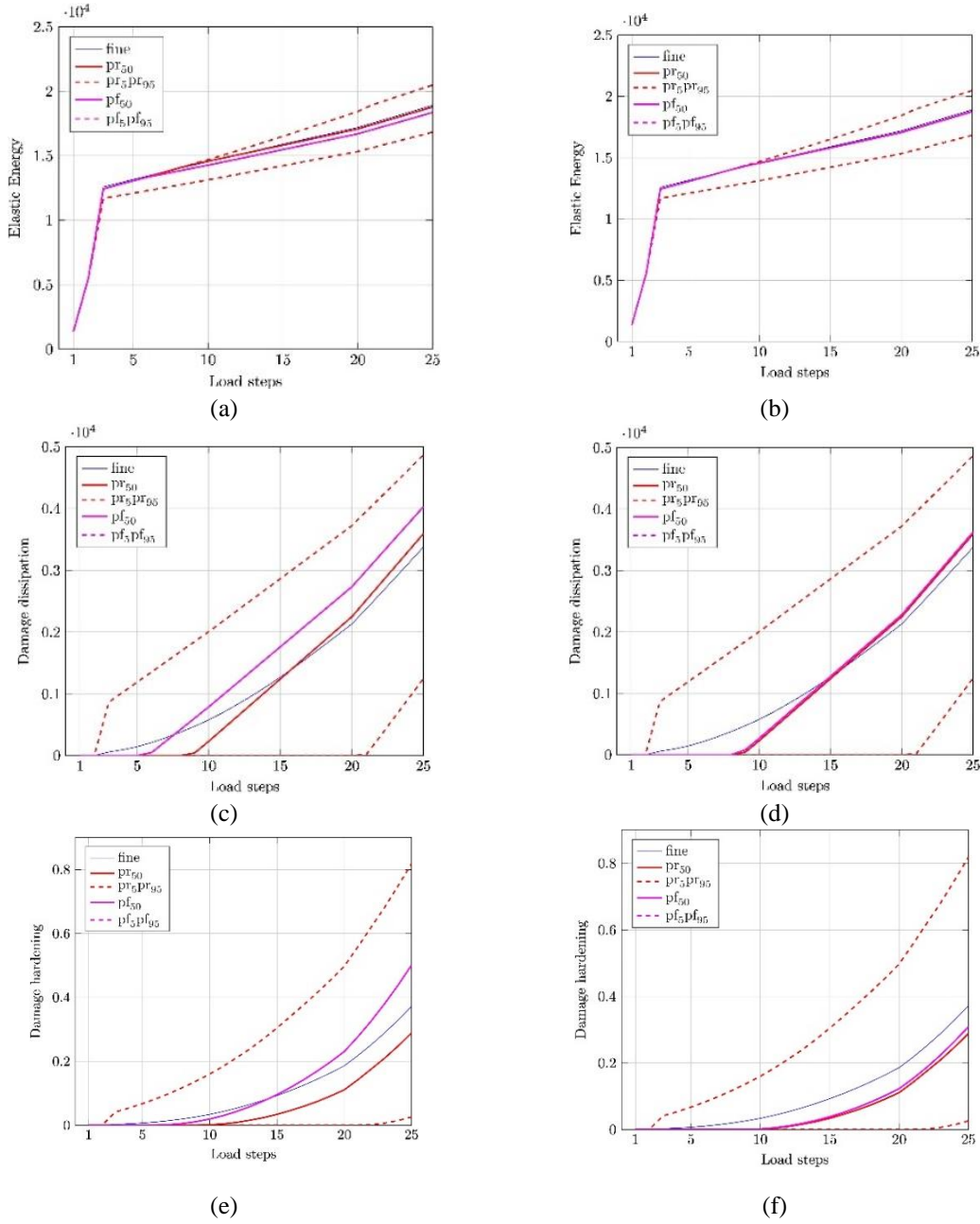


Fig. 12 Comparison of the percentile estimates of energy measures computed from the prior ( $pr_5, pr_{50}$  and  $pr_{95}$ ) and the updated ( $pf_5, pf_{50}$  and  $pf_{95}$ ) damage parameters with the fine-scale values using *sequential* (a), (c), (e) and *smoothing* (b), (d), (f) approaches

### 6.2.3 Update of damage parameters

The upscaling of the damage parameters  $\sigma_f$  and  $K_d$  is shown in Fig. 11. The corresponding loading program which triggers the damage phenomenon is depicted by Load IV in Fig. 6. By

validating the posterior predictive coarse-scale energies (elastic energy, damage dissipation and hardening) with the fine-scale counterpart in Fig. 12, one may conclude that updating performs comparatively better than *sequential* approach in a similar manner as in the plastic case.

## 7. Conclusions

In this paper, we have proposed a probabilistic approach to estimate unknown coarse-scale material parameters using fine-scale information. The material parameters on the coarse scale are considered random and are updated using fine-scale measurements in a Bayesian framework. To demonstrate the application of the proposed strategy, we considered the calibration of coupled damage-plasticity model on coarse scale. We used stored energy and dissipation to update the parameters governing the reversible and irreversible behaviour. The numerical examples were shown for homogeneous and heterogeneous fine scales. In case of homogeneous fine scale, the mean values of the coarse-scale parameters converge to their fine-scale counterpart with vanishing variation by performing loading experiments suitable for triggering different elastic and inelastic mechanisms. After validating the functioning of our approach and gaining knowledge about the loading cases conducive to identify material parameters, we turn to more realistic case of heterogeneous fine scale. In this case we performed the upscaling using *sequential* and *smoothing* approaches. By observing the comparison of different energy measures from the updated parameters with the fine-scale values, we can conclude that both approaches perform equally well for the elastic case. However, for plasticity and damage cases, in terms of matching stored hardening, the *sequential* approach performs better than the *smoothing* approach, whereas the latter performs better in terms of matching elastic energy and dissipation. The deviation between the coarse- and fine-scale energy responses for the inelastic phenomena can be attributed to a localized nature of the irreversible behavior on the fine scale which is understandably impossible to capture accurately with just one element on the coarse scale. This is substantiated by observing the severe jumps in the evolution of the update of inelastic parameters for the *smoothing* approaches. Nevertheless, the proposed approach provides a promising outlook to investigate further into the problems encountered in the heterogeneous case and to experiment with different fine- and coarse-scale models e.g., (Do and Ibrahimbegović 2015, Do *et al.* 2015, Ngo *et al.* 2014).

## Acknowledgments

This material is partially based upon the work supported by the DFG (Deutsche Forschungsgemeinschaft), Germany and the ANR (Agence Nationale de la Recherche), France under grant of the SELF-TUM project.

## References

- Arsigny, V., Fillard, P., Pennec, X. and Ayache, N. (2006), “Geometric means in a novel vector space structure on symmetric positive-definite matrices”, *SIAM J. Matr. Anal. Appl.*
- Asokan, B. and Zabarav, N. (2006), “A stochastic variational multiscale method for diffusion in heterogeneous random media”, *J. Comput. Phys.*, 654-676.
- Bobrowski, A. (2005), *Functional Analysis for Probability and Stochastic Processes*, Cambridge, Cambridge

- University Press.
- Brady, L., Arwade, S., Corr, D., Gutierrez, M., Breysse, D., Grigoriu, M. and Zabaras, N. (2006), “Probability and materials: From nano-to macro-scale: A summary”, *Probab. Eng. Mech.*, 193-199.
- Clément, A., Soize, C. and Yvonnet, J. (2013), “Uncertainty quantification in computational stochastic multiscale analysis of nonlinear elastic materials”, *Comput. Meth. Appl. Mech. Eng.*, 61-82.
- Del Maso, G., De Simone, A. and Mora, M. (2006), “Quasistatic evolution problems for linearly elastic perfectly plastic materials”, *Arch. Rat. Mech. Anal.*, 237-291.
- Demmie, P. and Ostaja-Starzewski, M. (2015), “Local and non-local material models, spatial randomness and impact loading”, *Arch. Appl. Mech.*
- Do, X.N., Ibrahimbegović, A. and Brancherie, D. “Localized failure in damage dynamics”, *Coupled Syst. Mech.*, **4**, 211-235.
- Do, X.N., Ibrahimbegović, A. and Brancherie, D. (2015), “Combined hardening and localized failure with softening plasticity in dynamics”, *Coupled Syst. Mech.*, **4**, 115-136.
- Evensen, G. (2009), *Data Assimilation-The Ensemble Kalman Filter*, Berlin, Springer.
- Gelman, A., Carlin, J., Stern, H. and Rubin, D. (2014), *Bayesian Data Analysis*, Boca Raton, Taylor and Francis.
- Ghanem, R. and Das, S. (2011), *Stochastic Upscaling for Inelastic Material Behavior from Limited Experimental Data*, Computational Methods for Microstructure-Property Relationships, Springer, Berlin.
- Gorguluarslan, R. and Choi, S.K. (2014), “A simulation based upscaling technique for multiscale modeling of engineering systems under uncertainty”, *J. Multisc. Comput. Eng.*, 549-566.
- Halpen, B. and Nguyen, Q. (1974), “Plastic and visco-plastic materials with generalized potential”, *Mech. Res. Commun.*, 43-47.
- Halpen, B. and Nguyen, Q. (1975), “Sur les matériaux standard généralisés”, *J. de Mécan.*, 39-63.
- Han, W. and Daya Reddy, B. (2013), *Plasticity, Mathematical Theory and Numerical Analysis*, Springer Verlag, New York, U.S.A.
- Hawkins-Daarud, A., Prudhomme, S., Van der Zee, K. and Oden, J. (2013), “Bayesian calibration, validation and uncertainty quantification of diffuse interface models of tumor growth”, *J. Math. Biol.*, 1457-1485.
- Ibrahimbegović, A. (2009), *Nonlinear Solid Mechanics*, Springer, Berlin.
- Ibrahimbegović, A. and Matthies, H.G. (2012), “Probabilistic multiscale analysis of inelastic localized failure in solid mechanics”, *Comput. Assist. Meth. Eng. Sci.*, 277-304.
- Ibrahimbegović, A., Gharzeddine, F. and Chorfi, L. (1998), “Classical plasticity and viscoplasticity models reformulated: theoretical basis and numerical implementation”, *J. Numer. Meth. Eng.*, 1499-1535.
- Ibrahimbegović, A., Markovic, D. and Gatuingt, F. (2003). “Constitutive model of coupled damage-plasticity and its finite element implementation”, *Rev. Européenn. Des Elem.*, 381-405.
- Kaipio, J. and Somersalo, E. (2004), *Statistical and Computational Inverse Problems*, Springer, Berlin.
- Kennedy, M. and O’Hagan, A. (2001), “Bayesian calibration of computer models”, *J. Roy. Stat. Ser. B*, 425-464.
- Koutsourelakis, P. (2007), “Stochastic upscaling in solid mechanics: An exercise in machine learning”, *J. Comput. Phys.*, 301-325.
- Liu, Y., Steven Greene, M., Chen, W., Dikin, D. and Liu, W. (2013), “Computational microstructure characterization and reconstruction for stochastic multiscale material design”, *Comput. Aid. Des.*, 65-76.
- Luenberger, D. (1969), *Optimization by Vector Space Methods*, John Wiley and Sons, Chichester.
- Markovic, D. and Ibrahimbegović, A. (2006), “Complementary energy based FE modeling of coupled elasto-plastic and damage behavior for continuum microstructure computations”, *Comput. Meth. Appl. Mech. Eng.*, 5077-5093.
- Matthies, H.G. (1991), “Computation of constitutive response”, In P. Wriggers, and W. Wagner, *Nonlinear Computational Mechanics: State of the Art*, Springer Verlag Berlin, Heidelberg.
- Matthies, H.G. (2007), “Uncertainty quantification with stochastic finite elements”, *Encyclop. Comput. Mech.*
- Matthies, H.G. and Ibrahimbegović, A. (2014), “Stochastic multiscale coupling of inelastic processes in solid mechanics. In M. Papadarakakis, and G. Stefanou”, *Multiscale Modelling and Uncertainty*

- Quantification of Materials and Structures*, Springer, Berlin.
- Matthies, H.G., Zander, E., Rosić, B., Litvinenko, A. and Pajonk, O. (2016), “Inverse problems in a Bayesian setting”, In A. Ibrahimbegović, *Computational Methods for Solids and Fluids-Multiscale Analysis, Probability Aspects, and Model Reduction*, Springer, Berlin.
- Ngo, V.M., Ibrahimbegović, A. and Brancherie, D. (2014), “Stress-resultant model and finite element analysis of reinforced concrete frames under combined mechanical and thermal loads”, *Coupled Syst. Mech.*, **3**, 111-144.
- Ngo, V.M., Ibrahimbegović, A. and Hajdo, E. (2014), “Nonlinear instability problems including localized plastic failure and large deformations for extreme thermomechanical load”, *Coupled Syst. Mech.*, **3**, 89-110.
- Nguyen, Q. (1977), “On the elastic plastic initial-boundary value problem and its numerical implementation”, *J. Numer. Meth. Eng.*, 817-832.
- Pajonk, O., Rosić, B., Litvinenko, A. and Matthies, H.M. (2012), “A deterministic filter for non-Gaussian Bayesian estimation-applications to dynamical system estimation with noisy measurements”, *Phys. D*, 775-788.
- Papoulis, A. (1991), *Probability Random Variables, and Stochastic Processes*, McGraw-Hill, New York, U.S.A.
- Pian, T. and Sumihara, K. (1984), “Rational approach for assumed stress finite elements”, *J. Numer. Meth. Eng.*, 1685-1695.
- Rosić, B. and Matthies, H.G. (2014), “Variational theory and computations in stochastic plasticity”, *Arch. Comput. Meth. Eng.*, 457-509.
- Rosić, B., Litvinenko, A., Pajonk, O. and Matthies, H.G. (2012), “Sampling-free linear Bayesian update of polynomial chaos representation”, *J. Comput. Phys.*, 5761-5787.
- Rosić, B., Sýkora, J., Pajonk, O., Kučerová, A. and Matthies, H.G. (2016), “Comparison of numerical approaches to Bayesian updating”, In A. Ibrahimbegović, *Computational Methods for Solids and Fluids-Multiscale Analysis, Probability Aspects and Model Reduction*, Springer, Berlin.
- Starzewski, M. (2008), *Microstructural Randomness and Scaling in Mechanics of Materials*, Boca Raton, Chapman and Hall.
- Stefanou, G., Savvas, D. and Papadrakakis, M. (2015), “Stochastic finite element analysis of composite structure based on material microstructure”, *Compos. Struct.*, 384-392.
- Steven Greene, M., Liu, Y., Chen, W. and Liu, W. (2011), “Computational uncertainty analysis in multiresolution material via stochastic constitutive theory”, *Comput. Meth. Appl. Mech. Eng.*, 309-325.
- Suquet, P. and Lahellec, N. (2014), *Elasto-Plasticity of Heterogeneous Materials at Different Scales*, Procedia IUTAM.
- Tarantola, A. (2005), *Inverse Problem Theory and Methods for Model Parameter Estimation*, SIAM, Philadelphia, U.S.A.
- Yvonnet, J. and Bonnet, G. (2014), “A consistent nonlocal scheme based on filter for the homogenization of heterogeneous linear materials with non-separated scales”, *J. Sol. Struct.*, 196-209.